

# DETECTION OF ECOSYSTEM FUNCTIONING USING OBJECT-BASED TIME-SERIES ANALYSIS

Wiebe Nijland<sup>a\*</sup>, Elisabeth A. Addink<sup>a</sup>, Steven M. de Jong, Freek D. van der Meer<sup>b</sup>

<sup>a</sup> Utrecht University, Department of Physical Geography, PO Box 80115, 3508 TC, Utrecht, The Netherlands.

\*Wiebe Nijland: geo.uu@wiebenijland.nl

<sup>b</sup> University of Twente, Faculty of Geo-Information Science and Earth Observation (ITC), Enschede, The Netherlands

**KEY WORDS:** Mediterranean, Vegetation, OBIA, Temporal, ASTER,

## ABSTRACT:

Accurate detection of tree growth and ecosystem functioning in naturally vegetated areas is of interest to many applications, such as ecological and land degradation modelling, wildfire risk monitoring, carbon budgeting, and climate science. However, the changes are often small when compared to normal spatial and seasonal variability, or occur gradually in time. We use object-based image analysis (OBIA) for time-series analysis of vegetation functioning because objects coincide better with ecological units in the field than pixels. For this study, we combine 12 ASTER images recorded between 2002 and 2008 with information from 75 field sites that were visited multiple times to provide field reference. A single segmentation of multi-temporal data is used to align all available data to a single object framework. The images are recorded before, during, and after the dry summer season, and thus show the effect of summer drought on the vegetation in our study area. The object-based method of creating time series from imagery allows for a reliable detection of small changes in NDVI and TIR. Using this approach, we show a differentiation in vegetation response to drought that can be related to the underlying lithological substrate and its water holding capacity. The presented method is especially valuable in fragmented landscapes which are common to areas in the Mediterranean basin.

## 1. INTRODUCTION

Changes in vegetation functioning are of great interest to many applications, such as ecological and land degradation modelling (Hoff and Rambal, 2003; Chiesi et al., 2002), wildfire risk monitoring (Maselli et al., 2000), carbon cycling (Pastor and Post, 1986), and climate science (Walther et al., 2002).

In this study we consider vegetation parameters at a canopy or ecosystem level, such as aboveground biomass, Leaf Area Index (LAI), light use and transpiration. These parameters represent vegetation functioning at different timescales: Biomass accumulates the growth over several decades; LAI changes at seasonal or yearly basis (Chason et al., 1991); while transpiration and light use have considerable variations depending on weather conditions and even the time of day (Gratani and Varone, 2004; Sala and Tenhunen, 1996).

Earth observation is a valuable tool for the monitoring of vegetation functioning and is the only feasible method to obtain spatially continuous data over large areas at regular intervals (Cohen and Goward, 2004). In the Peyne study area in Mediterranean France, we use earth observation to obtain detailed information on vegetation functioning on seasonal to yearly time scales to study the interaction of vegetation with the climate and landscape. The availability of multiple images acquired between 2002 and 2008 allows us to combine spatial, spectral, and temporal information in our analyses.

The changes of vegetation parameters due to stress or due to growth are often small when compared to the cyclic variations that occur at seasonal or daily timescales (Xiao et al., 2004; Richard and Pocard, 1998).

We use object-based image analysis (OBIA) for time-series analysis because objects better represent the ecological units in the field than pixels. The subtle changes in vegetation parameters are difficult to identify using traditional pixel based image analysis, because the pixel grid is an artificial regularization that is different for each image and therefore introduces additional unwanted variations to the data (Fisher, 1997). Therefore we use image segmentation to create a stationary object framework for our images to improve coupling between field and image data and to decrease the unwanted effects of pixel regularization and georectification errors.

For this study, we combine 12 images from the Advanced Spaceborne Thermal Emission and Reflectance radiometer (ASTER) (Yamaguchi et al., 1998) with information from 75 field sites that were visited multiple times to provide a field reference. At the field sites we measured aboveground biomass and LAI as principal vegetation parameters. LAI was measured both at the onset and near the end of the dry summer period in 2008, to record changes in leaf area. From the imagery we use NDVI as principal parameter, because of its relation to leaf area and light use (Tucker, 1979; Fensholt et al., 2004). As a second parameter we use thermal brightness, which is related to the surface energy balance and transpiration.

Within the extent of our study area in Mediterranean France, the natural vegetation cover is differentiated mainly by the variability in geological substrates. The focus of this paper is therefore on the relation between vegetation functioning and the geology at seasonal and inter annual timescales. The field sites were distributed over five common substrates which are used to stratify the data for further analyses. In this paper we

aim at gaining new insights in Mediterranean vegetation functioning and its relation with the geological substrates. We use the temporal patterns in LAI, NDVI, and thermal brightness as key parameters on vegetation functioning. The application of OBIA is an important factor in this process, because it allows detection of small changes in thermal radiance and NDVI, and provides a reliable coupling between field and image data.

## 2. METHODS

### 2.1 Study Area:

The study area is part of the Payne catchment, situated in Mediterranean France. The region has a Mediterranean sub-humid climate with annual average precipitation of 800–1000 mm and a dry summer season. The catchment is situated at the edge of the ‘Montagne Noir’ and is characterized by a high spatial variation of bedrock material because the formations were tilted and heavily deformed during the Hercynian orogenesis (Alabouvette, 1982). Common types of bedrock are limestone, basalt, flysch, calcareous sandstone, and dolomite. Soils in the area are shallow and are poorly developed with often only an AC or AR profile. Soil characteristics are differentiated mainly upon the nature of the geological substrate (Bonfils, 1993).

Part of the study area is used for agriculture, mostly vineyards and pasture. The steep hills, remote areas, and poorest soils are covered with (semi)natural vegetation ranging between low (< 0.5 m) herbs and shrub, and moderate (< 10 m) evergreen forests. The dominant tree and shrub species are *Quercus ilex*, *Arbutus unedo*, *Erica arborea*, and *Buxus sempervirens*; these are all evergreen and sclerophyllous. Much of the area has been cultivated as coppices in the past (Mather et al., 1999), which has resulted in many small stems sprouting from a shared root system. Tree height varies between 1 to 10 m with little or no understory vegetation.

### 2.2 Imagery

For this study we use 12 ASTER scenes recorded between 2002 and 2008. The images were preprocessed by JPL into surface reflectance for the Visual and Near InfraRed (VNIR) sensor and into surface radiance for the Thermal InfraRed (TIR) sensor (Abrams and Hook, 2008). The pixel size is 15 m for VNIR and 90 m for TIR. The VNIR bands are used to obtain the NDVI which is related to vegetation cover, LAI, and the photosynthetic activity of the vegetation. The TIR information is closely related to the surface temperature which is influenced by the cooling effect of transpiration of the vegetation, and by the emissivity of the surface (Schmugge et al., 2002). The SWIR bands were not used because they are unavailable for 2008 as a result of a sensor defect.

To ensure a good geographical correspondence between the field locations and the imagery, the image of 20070814 was georeferenced using 70 ground control points. All other images are corrected using image-to-image registration to this reference image based on > 300 evenly spread tie-points. The location accuracy of all images is close to

1 pixel (15m). All images were cropped to a size of 1550 by 1250 pixels and cover the area between 0512083–4836478 and 0535333–4817728 (UTM31N, WGS84). The TIR bands were resampled to the 15m grid using the nearest-neighbour method to preserve the original values without smoothing.

### 2.3 Image Segmentation:

To improve the coupling between the field data and the images and because objects coincide better with ecological units in the field than pixels, we used object-based image analysis (OBIA) for the stacked time-series of images. OBIA strengthens the signal and reduces errors due to spatial mismatches and canopy illumination differences. A single multi-scale segmentation was applied to the multi-temporal data to align all data to a single object-based framework. Because the VNIR and TIR bands have different spatial sampling resolutions, we use hierarchical multi-scale image segmentation with two levels. The first level is optimized for the VNIR bands and in the second level the segments are aggregated into larger units optimized for the TIR bands. Further analyses of the spectral data and temporal dynamics were based on the spatially averaged spectral values of the objects obtained by image segmentation.

The multi-scale hierarchical segmentation was applied to the stacked ASTER images using the eCognition Developer 8 (Definiens, 2009) software package. Three images with partial cloud cover were excluded from the segmentation because the clouds would interfere with the segmentation. The remaining images got equal weights in the segmentation.

The segmentation parameters were chosen with two main objectives: 1) To obtain one common spatial framework for the analysis of multitemporal data, minimizing then effects of the regularization imposed by the sensor and faults in the image geographical registration. 2) To create spectrally homogeneous objects that represent the spatial structure of the landscape and more specifically the variability within the naturally vegetated areas.

In previous research in the Payne area, we determined the optimal support size for spectral studies on natural vegetation. The size was found to be between 1300 and 2500 m<sup>2</sup> for square pixels (Nijland et al., 2009) and between 6300 and 8500 m<sup>2</sup> for image based segments (Addink et al., 2007). Based on these results we aimed at an average segment size of 7500 m<sup>2</sup> for the areas with full forest cover (NDVI > 0.8). The selection of the forest area only was done because the optimum in these studies was found for natural vegetation which mainly covers the more homogeneous parts of the landscape.

For the TIR bands, the 7500 m<sup>2</sup> segments were too small because they cover less than one original 90 m pixel. To get a stable statistical description of a segment it needs to be several times the size of an original pixel (Strahler et al., 1986). We took 10 TIR pixels (81000 m<sup>2</sup>) as the modal segment size to assure that all segments would be large enough. The segments in the more homogeneous, forested areas are generally larger, with an average size of 162000 m<sup>2</sup> for segments with NDVI > 0.8.

Table 1: Allometric relations for aboveground biomass calculations

| Species                                   | Formula   | Source              |
|---|---|---------------------|
| <i>Arbutus unedo</i>                      | $\ln AB = 4.251 + 2.463 * \ln D50$                  | Ogaya et al. 2003   |
| <i>Quercus ilex</i>                       | $\ln AB = 4.900 + 2.277 * \ln D50$                  | Ogaya et al. 2003   |
| Shrubs (stem $\varnothing < 3\text{cm}$ ) | $AB = 642.0 * H^{0.0075} * D_{\text{max}}^{2.4901}$ | Pereira et al. 1994 |

AB : Aboveground biomass individual [g]

D : Diameter [cm] (D50: Stem diameter at 50cm, Dmax : maximum projected shrub diameter)

H: Height [m]

In both segmentation levels the weight of the segment shape was set to 0.2 using compactness only. The spectral information gets the largest weight to obtain homogeneous segments, but compactness is included because compact segments are more robust with respect to variability at the edges of the segments which is introduced spatial misalignment of the images.

### Field data

Field data were collected in 2008. For this study, we have 75 field plots which were all visited twice: in June, at the onset of the dry summer period; and in September, near the end of the dry season. At each site we measured the diameter of all tree stems in a 5x5 meter square sample plot and made a series of five hemispherical photographs for the calculation of LAI. At the second visit, only the LAI was determined because the changes in stem diameter over one season are not significant

LAI is defined as the one-sided leaf-area per unit ground area (Watson, 1947). The hemispherical photographs were taken at the four corners and in the centre of each field plot and the LAI was determined using Can-Eye software (Weiss et al., 2004; Jonckheere et al., 2004).

Aboveground biomass was estimated using allometric relations between stem diameter and biomass. Allometric relations for trees were available for *A.unedo* and *Q.ilex* (Ogaya et al., 2003). The other tree species were divided into two groups, based on morphological similarity to either *A.unedo* or *Q.ilex*. Biomass was estimated using the respective relation (table 1). For the shrub species a generic formula for Mediterranean shrubs was used based on the maximum diameter and height per individual (Pereira et al., 1994). The biomass of all individuals were summed per plot and recalculated to  $\text{kg} * \text{m}^{-2}$ .

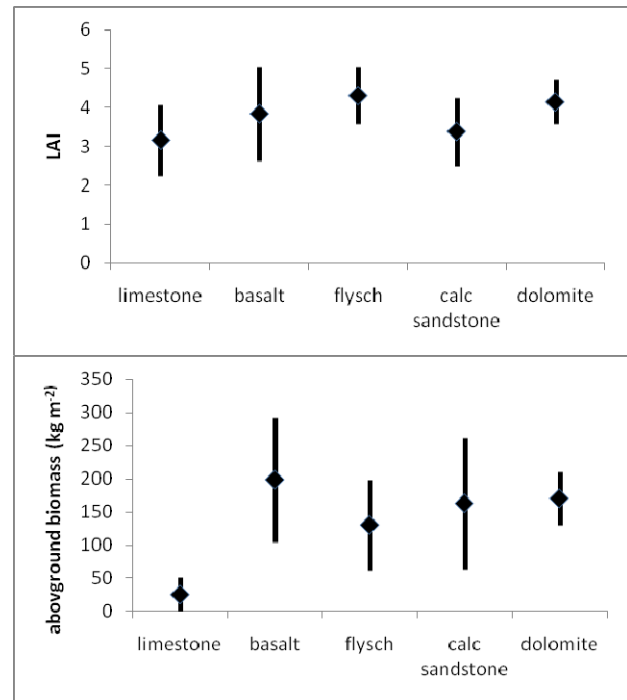


Figure 1: Average values and one sd of A: aboveground biomass and B: LAI of the five main substrates

### 3. RESULTS

The field plots were situated in five of the most important substrates of the study area. The substrates are the basic units for further analyses and the average values and standard deviations of LAI and aboveground biomass are shown in figure 1. The limestone has a low shrub type vegetation and therefore considerably lower aboveground biomass than the other substrates that have a forest cover. The calcareous sandstone and flysch substrate have a dense forest cover with a closed canopy. Since the trees were coppiced in the past they have no real stems. Instead they branch out from stools resulting in thin stems only resulting in relatively low values for aboveground biomass.

Image spectra were collected at all field plot locations. As a reference we added a bare dolomite mine, and an area with grass cover to the plots of NDVI and TIR over time (figure 2). To emphasize the thermal differences within the study area and to reduce the effect of large temperature fluctuations, the TIR data is presented as a percentage of the water thermal radiance.

The thermal brightness of the lake area is plot in the graph and set by definition at 100%. The year, month and day of image acquisitions are noted at the horizontal axis of the graphs.

The most striking feature is the strong reduction of NDVI and rise of temperature of the grass area over the course of summer. The mine is completely bare and has a low NDVI and strong thermal radiance, although not as strong as the grass area because of its high albedo. The naturally vegetated areas have similar behaviour at first sight, but at closer look the limestone and basalt have stronger reduction in NDVI and temperature rise then the other substrates.

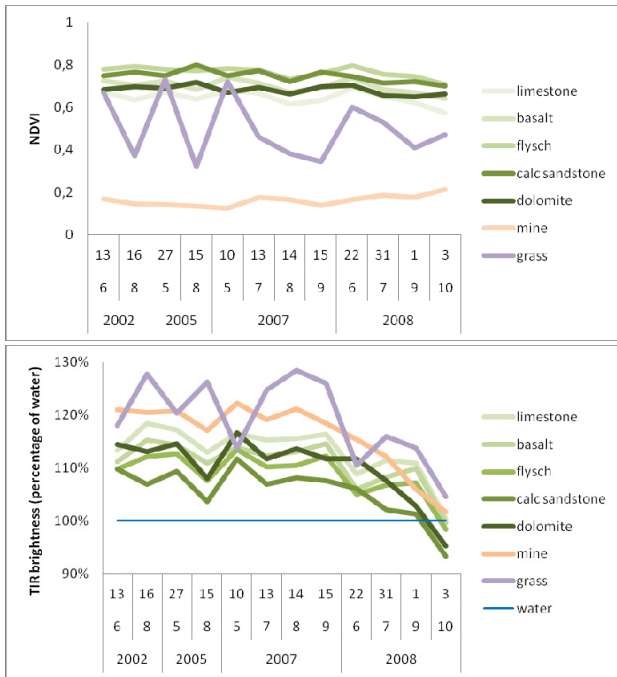


Figure 2: Average values of ASTER images for vegetated segments and an active open dolomite mine through time for A: NDVI and B: TIR surface rightness relative to the lake area.

**Dry season**

In 2008 we had two field campaigns, one in June and one in September. In each campaign we visited the same 75 plots to record changes in LAI during the dry summer season. The vegetation is evergreen, but in dry circumstances part of the leaves may be shed. In 2008, the dry season started at the end of June, and lasted three months. During this period there is very little rainfall, and the trees depend entirely on water extracted from the ground. The type of substrate determines the water holding capacity and the depth of fissures that allow tree roots to reach this water. The changes of LAI determined in the field, and NDVI and TIR derived from ASTER from June to September are shown in figure 3.

The limestone and basalt area show a reduction in LAI and NDVI and an increase in TIR. These areas show clear signs of stress, and shedded part of their leaves. This results in a reduction of NDVI and in a reduced transpiration, leading to higher surface temperatures. The calcareous sandstone and dolomite areas show no reduction in LAI and dolomite even an

increase in LAI. This is consistent with a smaller reduction in NDVI and lower TIR values indicate that vegetation on these substrates was less stressed and had less reduction in transpiration. The flysch area is indifferent and shows a mixed signature with little reduction in LAI and NDVI, but an increase in TIR. This could mean that transpiration is already reduced because of water shortage, but leaf shedding has not yet occurred.

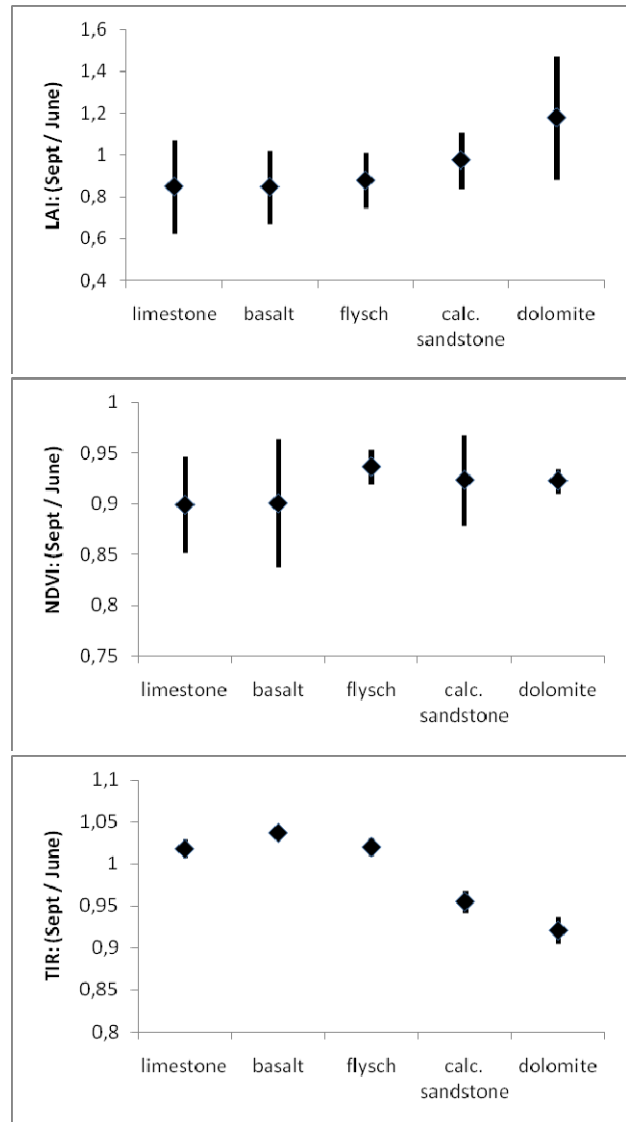


Figure 3: Differences between June and September values for A: LAI, B: NDVI and C: TIR for 2008 with the bars indicating the standard deviation of the plots.

**4. DISCUSSION**

With the combination of spectral and temporal information from earth observation we investigate the vegetation functioning at different lithological substrates in the Peyne study area. The use of multi-temporal data introduces a number of issues regarding the spatial and spectral correction of the used images. Although all images were acquired by the same sensor and were processed in a standardized, validated manner

by JPL, still some differences between the images need to be considered when interpreting the data. The VNIR reflectance of the open and active dolomite mine should be constant, but small variability is still present.

To reduce the effects of small scale (~pixel size) variability and spatial misalignment of the images, we use image segmentation to create a stationary object framework for the time series analyses. The use of one object framework derived from the stacked image time-series also improves the coupling between field and image data, because the support of the image data is enlarged and more constant through time when compared to a pixel based approach.

The spectral corrections of the VNIR reflectance images were effective as is shown by the NDVI of the dolomite mine (fig 2a). The mine is actively exploited and has a constant bare dolomite surface. The temporal stability of this surface can be used as a reference and shows a reasonably stationary signal. The remaining signal might be noise in the NDVI values, because the dolomite mine has a spectral flat response throughout the spectrum and hence very low NDVI values.

We normalized the TIR information to the radiance taken from two artificial lakes in the study area. The water temperature of the lakes is not constant and shows a delayed change compared to temperature changes over land. However, by comparing the vegetated areas to the water, we obtain information about the transpiration of the vegetation and its difference with an ideal open-water, evaporating surface. On a wet area or healthy vegetation, much of the incoming energy is used to evaporate water which will have a cooling effect on the surface. Vegetation with water shortage has less transpiration leading to higher surface temperatures. Apart from temperature, the TIR radiance depends also on the emissivity of the surface. There was no need to correct for emissivity changes, because they can be considered constant through the year for a closed forest cover (Schmugge et al., 2002). The emissivity of the pasture may decrease when the grass dries, therefore temperature changes may be somewhat larger than already shown here.

The main focus of this study was on the shrub and forest vegetations in our study area but it is difficult to separate the effects of stress on evergreen vegetation from the seasonality of grasses and annuals. In the flysch and calcareous sandstone, the canopy cover is almost continuous and herb cover is absent, but in the dolomite and even more at the basalt and limestone there is considerable grass cover between or under the trees. In these locations, the seasonal change of the grass cover influences the temporal patterns of NDVI and transpiration and partly obscures the changes in the trees and shrubs.

## 5. CONCLUSIONS

In this paper we presented an object based analysis of multi-temporal remotely sensed and field data aimed at monitoring vegetation functioning and especially the effects of drought stress during the summer. Looking at five substrates in our study area, we found differences in our key indicators for vegetation health -LAI, NDVI, and TIR- that can be related to the resilience of the vegetation against summer drought. The

relation between these vegetation patterns and the geological substrates in our study area indicates the importance of soil water storage on vegetation growth.

In this study we used an object-based method of creating temporal units from imagery because it allows for a stable coupling between field and image data. The object-based analysis decreases the effects of edge, and image misalignment. The presented method using object based analysis of high resolution images is especially valuable in fragmented landscapes with a high spatial variability of the environmental conditions, which is common in Mediterranean areas.

## REFERENCES

- Abrams., M, and S. Hook. 2008. ASTER user handbook version 2. Jet Propulsion Laboratory, Pasadena. <http://asterweb.jpl.nasa.gov>
- Addink, E.A., S.M. De Jong, and E.J. Pebesma. 2007. The importance of scale in object-based mapping of vegetation parameters with hyperspectral imagery. *Photogrammetric Engineering and Remote Sensing* 73, no. 8: 905-912.
- Alabouvette, B., 1982. Carte Géologique de la France 1:50 000. Feuille Lodève; BRGM, Orléans
- Bonfils, P., 1993. Carte Pédologique de la France 1:100 000; Feuille Lodève. INRA, Olivet
- Chason, Jennifer W., Dennis D. Baldocchi, and Michael A. Huston. 1991. A comparison of direct and indirect methods for estimating forest canopy leaf area. *Agricultural and Forest Meteorology* 57, no. 1-3 (December): 107-128
- Chiesi, M., F. Maselli, M. Bindi, L. Fibbi, L. Bonora, A. Raschi, R. Tognetti, J. Cermak, and N. Nadezhkina. 2002. Calibration and application of FOREST-BGC in a Mediterranean area by the use of conventional and remote sensing data. *Ecological Modelling* 154, no. 3: 251-262.
- Cohen, W.B., and S.N. Goward. 2004. Landsat's role in ecological applications of remote sensing. *BioScience* 54, no. 6: 535-545.
- Definiens, 2009. e-Cognition. <http://www.ecognition.com>
- Fensholt, R., I. Sandholt, and M.S. Rasmussen. 2004. Evaluation of MODIS LAI, fAPAR and the relation between fAPAR and NDVI in a semi-arid environment using in situ measurements. *Remote Sensing of Environment* 91, no. 3-4: 490-507.
- Fisher, P., 1997. The pixel: A snare and a delusion. *International Journal of Remote Sensing* 18, no. 3: 679-685.
- Gratani, L., and L. Varone. 2004. Adaptive photosynthetic strategies of the Mediterranean maquis species according to their origin. *Photosynthetica* 42, no. 4: 551-558.
- Hoff, C., and S. Rambal. 2003. An examination of the interaction between climate, soil and leaf area index in a *Quercus ilex* ecosystem. *Ann. For. Sci* 60: 153-161.
- Jonckheere I., S. Fleck, K. Nackaerts, B. Muysa, P. Coppin, M. Weiss, and F. Baret. 2004. Review of methods for in situ leaf

- area index determination Part I. Theories, sensors and hemispherical photography. *Agricultural and Forest Meteorology* 121: 19-35.
- Llorens, L., J. Peñuelas, and I. Filella. 2003. Diurnal and seasonal variations in the photosynthetic performance and water relations of two co-occurring Mediterranean shrubs, *Erica multiflora* and *Globularia alypum*. *Physiologia Plantarum* 118, no. 1: 84-95.
- Maselli, F., A. Rodolfi, L. Bottai, S. Romanelli, and C. Conese. 2000. Classification of Mediterranean vegetation by TM and ancillary data for the evaluation of fire risk. *International Journal of Remote Sensing* 21, pp. 3303-3313.
- Mather, A.S., J. Fairbairn, and C.L. Needle. 1999. The course and drivers of the forest transition: the case of France. *Journal of Rural Studies* 15, pp. 65-90.
- Nijland, W., E.A. Addink, S.M. De Jong, and F.D. Van der Meer. 2009. Optimizing spatial image support for quantitative mapping of natural vegetation. *Remote Sensing of Environment* 113, no. 4: 771-780.
- Ogaya, R., J. Peñuelas, J. Martínez-Vilalta, and M. Mangirón. 2003. Effect of drought on diameter increment of *Quercus ilex*, *Phillyrea latifolia*, and *Arbutus unedo* in a holm oak forest of NE Spain. *Forest Ecology and Management* 180, no. 1-3: 175-184.
- Pastor, J., and W.M. Post. 1986. Influence of climate, soil moisture, and succession on forest carbon and nitrogen cycles. *Biogeochemistry* 2, no. 1: 3-27.
- Pereira, J.M.C., T.M. Oliveira, and J.P.C. Paul. 1994. Fuel mapping in a Mediterranean shrubland using Landsat TM imagery; In: Kennedy, P.J. and Karteris, M. (Eds.) *Proc. International Workshop on Satellite technology and GIS for Mediterranean forest mapping fire management* (pp 97-106). Office for Official Publications of the European Communities, Luxembourg.
- Richard, Y., and I. Pocard. 1998. A statistical study of NDVI sensitivity to seasonal and interannual rainfall variations in Southern Africa. *International Journal of Remote Sensing* 19, no. 15: 2907-2920.
- Sala, A., and J. D. Tenhunen. 1996. Simulations of canopy net photosynthesis and transpiration in *Quercus ilex* L. under the influence of seasonal drought. *Agricultural and Forest Meteorology* 78, no. 3-4: 203-222.
- Schmugge, T., A. French, J.C. Ritchie, A. Rango, and H. Pelgrum. 2002. Temperature and emissivity separation from multispectral thermal infrared observations. *Remote Sensing of Environment* 79, no. 2-3: 189-198.
- Strahler, A.H., C.E. Woodcock, and J.A. Smith. 1986. On the nature of models in remote sensing. *Remote Sensing of Environment* 20, no. 2: 121-139.
- Tucker, C.J. 1979. Red and photographic infrared linear combinations for monitoring vegetation. *Remote Sensing of Environment* 8, no. 2: 127-150.
- Walther, G.-R., E. Post, P. Convey, A. Menzel, C. Parmesan, T.J.C. Beebee, J.-M. Fromentin, O. Hoegh-Guldberg, and F. Bairlein. 2002. Ecological responses to recent climate change. *Nature* 416, no. 6879: 389-395.
- Watson, D. J., 1947. Comparative physiological studies in the growth of field crops. I. Variation in net assimilation rate and leaf area between species and varieties, and within and between years. *Ann. Bot.* 11: 41-76.
- Weiss, M., F. Baret, G.J. Smith, I. Jonckheere, and P. Coppin. 2004. Review of methods for in situ leaf area index (LAI) determination Part II. Estimation of LAI, errors and sampling. *Agricultural and Forest Meteorology* 121: 37-53.
- Xiao, Xiangming, Qingyuan Zhang, Bobby Braswell, Shawn Urbanski, Stephen Boles, Steven Wofsy, Berrien Moore, and Dennis Ojima. 2004. Modeling gross primary production of temperate deciduous broadleaf forest using satellite images and climate data. *Remote Sensing of Environment* 91, no. 2: 256-270.
- Yamaguchi, Y., A.B. Kahle, H. Tsu, T. Kawakami, and M. Pniel. 1998. Overview of advanced spaceborne thermal emission and reflection radiometer (ASTER). *IEEE Transactions on Geoscience and Remote Sensing* 36, no. 4: 1062-1071.